This is a repository copy of *Static behaviour of two-tiered Dou-Gong system reinforced by super-elastic alloy*.

Accepted manuscript

As a service to our authors and readers, we are putting peer-reviewed accepted manuscripts (AM) online, in the Ahead of Print section of each journal web page, shortly after acceptance.

Disclaimer

The AM is yet to be copyedited and formatted in journal house style but can still be read and referenced by quoting its unique reference number, the digital object identifier (DOI). Once the AM has been typeset, an 'uncorrected proof' PDF will replace the 'accepted manuscript' PDF. These formatted articles may still be corrected by the authors. During the Production process, errors may be discovered which could affect the content, and all legal disclaimers that apply to the journal relate to these versions also.

Version of record

The final edited article will be published in PDF and HTML and will contain all author corrections and is considered the version of record. Authors wishing to reference an article published Ahead of Print should quote its DOI. When an issue becomes available, queuing Ahead of Print articles will move to that issue's Table of Contents. When the article is published in a journal issue, the full reference should be cited in addition to the DOI.

1

Manuscript title: Static Behaviour of Two-Tiered Dou-Gong System Reinforced by Super-Elastic Alloy

Authors: Wenjun Xie[1], Tsung-Hsien Wang[2], Wen-Shao Chang[2]

Affiliations: [1]Department of Architecture and Civil Engineering, University of Bath, Bath, UK.

[2]Sheffield School of Architecture, The University of Sheffield, Sheffield, UK.

Corresponding author: Wen-Shao Chang, Sheffield School of Architecture, Arts Tower, The University of Sheffield, Sheffield, S10 2TN, UK . Tel.: +44 1225384020

E-mail: w.chang@sheffield.ac.uk

Abstract

Dou-Gong system in Asian timber structures play an important role in resisting seismic action. Traditional carpentry in Asia uses timber pegs to connect components which enables relative movement between components, and hence provide friction to dissipate energy in an earthquake. This method however has some short falls such as inadequate stiffness to resist large lateral force and therefore the structures tend to exhibit permanent deformation after the earthquakes. This study proposes a new technique by using super-elastic alloy bars to replace the conventional wooden peg connections to enhance the seismic performance of the structures. Static push-over experiments were conducted on full scaled two-tiered Dou-Gong systems and the high-strength steel and conventional wood pegs as benchmarks. The ultimate stiffness of Dou-Gong system has shown increase by using both high-strength steel and super-elastic alloy bars, but only super-elastic alloy can provide a consistent high damping ratio. This technique also involves pre-strain the super-elastic alloy and the outcomes of this series of experiments have shown that pre-strain in the super-elastic alloy can significantly increase the damping ratio in the structure and hence more energy is dissipated. The results of this paper can be used in the projects of timber structures with Dou-Gong system.

3

Notation

W is the weight on top of the structure

ζ is the equivalent damping ratios

A_h is the dissipated energy in one loading cycle

A_e is the maximum elastic strain energy in one loading cycle

4

1. Introduction

The existing oriental timber buildings which have a long history are often considered the cultural heritage of a country. A large proportion of these buildings are situated in the seismic belts in East Asia and thus there is a critical need for conservation against earthquakes and other forms of natural disaster. These timber buildings have diverse connection systems, such as dovetail connections (Chang & Hsu, 2005) and Dou-Gong system. The anti-seismic performance of historic timber buildings has been extensively studied over the past 20 years (Fang et al., 2001a; Fang et al., 2001b; Fujita, Hanazato & Sakamoto, 2004; Chang, 2005; Suzuki & Maeno, 2006; Chang, Hsu & Komatsu, 2006; Chang & Hsu, 2007; Yu et al., 2008; Chang et al., 2009; Xue et al., 2015; Yeo et al., 2018; Xie, Araki & Chang, 2018), and it has been recognised that Dou-Gong systems in historic timber buildings play an important role in resisting seismic action. Dou-Gong systems are located at the top of columns to support upper structures and transmit the weight of both the structures and the roof to the columns and the foundations. The fundamental elements of a Dou-Gong system are the Dou (斗), Gong (拱) and Ang (昂), as shown in Figure 1. The Dou is a rectangular timber element with a cross groove at its upper side. Gong and Ang are timber elements placed onto the cross groove of the Dou perpendicular and parallel respectively to the beams. Dou are connected to the lower elements by a wooden peg (Figure 2).

Both static and dynamic experiments and analysis have been conducted by many researchers who have confirmed the non-linear stiffness of Dou-Gong (Fujita et al, 2000; Suzuki & Maeno, 2006; Tsuwa et al., 2008; Fujita et al., 2008; Hwang et al., 2008; Yeo et al,

5

2016a; Yeo et al., 2016b). The rotation of base Dou often experiences major horizontal deformation in the region of initial stiffness. Sliding has been observed when the horizontal load exceeds the frictional capacity between the elements and this has resulted in the lower second stiffness. The Dou-Gong system dissipates most of the energy through the sliding and movements between each element.

Although the Dou-Gong system has a self-centring nature and can undergo large deformations, many historical buildings have been seriously damaged or have collapsed in the event of an earthquake due to the low strength and stiffness of the Dou-Gong system. For example, during the 1999 Chi-Chi earthquake in Taiwan, 42% of traditional timber structures were seriously damaged and 48% collapsed, whereas only 10% of other buildings were damaged (Chang, 2005). Enhancing the seismic performance of the Dou-Gong system is therefore the primary task that needs to be focused upon but has yet to be started in earnest.

Two fundamental advantages the Dou-Gong system provides to ensure good anti-seismic performance are re-centring capability and energy dissipation capacity. Re-centring capability is driven by the re-centring force which pulls the oblique structure back to its original position. The weakest point of the Dou-Gong system is the conventional wooden peg which, after an earthquake, is either pulled out from the hole or exhibits permanent deformation. A simple technique has been developed whereby metal bars are used to replace the conventional wooden peg connections to enhance the seismic performance of base Dou. It achieves this by maintaining base Dou's original re-centring capability and increasing both its energy dissipation capacity and its ultimate strength (Xie, Araki & Chang, 2018).

6

This paper reports push-over experiments conducted on Dou-Gong systems with two tiers. Tests were conducted with conventional wooden peg connections and two metal connections (high strength steel and super-elastic alloy).

2. Experimental method

A full-scale replica of a two-tiered Dou-Gong system, which duplicates a historical building in Sichuan Province in China, was made of glued laminated timber. The conventional connections of Dou and the lower structure were wooden pegs. The tests involved using high strength steel and a super-elastic alloy to replace the wooden pegs to improve the seismic performance of the Dou-Gong system. Push-over tests were then conducted where the lateral loads were applied using a hydraulic jack. The displacements and rotations of components of the Dou-Gong system were measured by 18 LVDTs. Moment versus rotation curves were then obtained to evaluate the seismic performance.

2.1 Materials

The material used to make the Dou-Gong system was glulam GL28h and its mechanical properties are listed in Table 1. Apart from the Gong and Ang which connect by interlocking, the conventional wooden pegs that connect Dou and the lower structure were also made using GL28h. The reason for the use of glulam was due to the limitation of accessing large sectioned sawn timber to make the specimens.

Two materials, high strength steel and super-elastic alloy bars (as shown in Figure 3), were used to replace the wooden pegs. The original diameter of the bars was 12mm. The

middle part of the bar was machined down to 6mm to lower the pre-strain load on the timber

and threads of M8 and M12 were located at each end. The length of the reduced section was

105mm for the base Dou connection and 60mm for upper Dou connections.

The super-elastic alloy is a smart material known as a shape memory alloy because its

shape memory effect has been widely used in many different fields, including civil structures,

automotive, aircraft, and medicine. The materials used in this research have a super-elasticity

effect. The nature of the materials and their two different effects is schematised in Figure 4

(Chang & Araki, 2016). The material has two crystal structures austenite and martensite, which

can be transferred to each other by changing the temperature of the material and altering the

external stress. M_f, M_s, A_s and A_f denote the start and finish transformation temperature points

between martensite and austenite phases and are set during the manufacture of the materials.

The super-elastic alloy used in this research was provided by Furukawa Techno Material Co.,

Ltd. Japan has a transformation temperature, A_f, of -39°C which is much lower than the

ambient temperature of most regions in the world, especially within the area in which the

historic timber buildings are distributed. This material therefore has a super-elasticity effect

that can invoke phase transformations by changing the external stress.

A pre-strain (Figure 5) can be applied to the super-elastic alloy bar by applying an axial

tensile force onto the bar. This will change the initial crystal structure of the connection bar to

detwinned martensite and theoretically omit the initial elastic stage and thus dissipate energy

more quickly.

The high strength steel bar was tested axially and yielded an ultimate strength of 720

8

MPa, much higher than that of the super-elastic alloy bar. However, the high strength steel bar

fractured at 3.6% strain. There was negligible residual strain of the super-elastic alloy bar after

tensile tests up to 7% strain. Figure 6 compares the stress-strain curve of high strength steel bar

and the super-elastic ally bar. The chemical composites of the super-elastic alloy used in this

research were copper (81.84wt%), aluminium (7.43wt%) and manganese (10.74wt%) which

were measured using a Scanning Electron Microscope.

2.2 Dou-Gong specimen and structure set up

This two-tiered Dou-Gong system consisted of 11 individual components including the timber

block that represents the top of a column. The lower layer comprised a base Dou, one Gong,

and one Ang. The upper layer comprised 4 small Dou, 3 Gongs, and one Ang. Each Dou was

connected to the lower structure by a wooden peg. There are two types of wooden peg

connection, dovetail and flat cut. The pull-out force is independent of the dead load when the

dovetail connection is used but changes along with the dead load when a flat cut connection is

used. In this research, the flat cut wooden peg connections were applied. The dimensions were

28 x 28 x 56mm for the base Dou connection and 26 x 26 x 52mm for the upper layer Dou

connections.

The timber block that represents the top of the column was fixed to the strong floor by

two 24mm threaded bolts. Two angle plates were also fixed to the strong floor to prevent the

timber block from sliding.

The two-tiered Dou-Gong system was placed on top of the block in sequence, as shown

in Figure 7. Gong and Ang were fitted in the grooves of Dou and bonded together. Five Dous

9

were connected to the lower structures by wooden pegs or metal bars. Cubic holes with a width

of 28mm were chiselled out for the wooden pegs in both the bottom of base Dou and the top of

the timber block while 26mm width holes were chiselled out in the bottom of four upper Dou

and the top of the corresponding elements.

As Figure 8 shows, a simple system was developed for the metal bar connections. 12mm

thread inserts (Figure 8a) were fixed into the timber block, first level Gong, and Ang using

epoxy resin. The metal bar was placed first and inserted through the centre of the Gong along a

pre-drilled vertical hole. A 100mm square steel plate and 50mm diameter washers were then

embedded in the top surface of the base Dou and upper level Dou respectively to prevent

damage to the timber caused by axial loads from the bar. A ball joint was then placed on top to

remove the rotational restraint and provide a pin joint to the connection system. The top end of

the connection system was fixed by a nut, which in some cases gives the pre-strain load to the

super-elastic bar. This connection system is shown in detail in Figure 8c.

Eight LVDTs (No. 1 to 8) were attached to the first level Gong and Ang to measure the

sliding displacements and rotations of four upper level Dou. Two sets of four LVDTs (No. 9 to

16) were placed vertically to measure the total rotations and base Dou rotations, respectively.

The radian of each rotation was calculated by the differences in the measurement of LVDTs on

the left and right sides, as shown in Figure 9. Two horizontal LVDTs (No. 17 and 18) measured

the horizontal sliding displacement of both base Dou and the entire structure. A pallet was

fixed on top of the Dou-Gong to house the concrete blocks and simulate the vertical load

exerted on the structure. The lateral loads were applied by a hydraulic jack fixed onto the wall.

The vertical distance from the loading point to the bottom level of base Dou was 700mm. The

setup details for this structure are shown in Figure 9.

2.3 Test programme

For historic buildings, the weight of the roof plays a very important role in the structure and

can often vary. To simulate this, 400, 700, and 1000kg weights were applied to the top of the

structure to explore how the weight of the roof changes the behaviour of the structure.

As listed in the test protocol (Table 2), three different materials connecting the Dou and

the lower elements under three weight levels were applied. One loading cycle was defined as

the trajectory of the Dou-Gong system that rotates to a certain point with a prescribed radian

and recovers to its original position. The three prescribed radians were 0.05, 0.06 and 0.07 and

the Dou-Gong system loaded 3 cycles for each radian. Thus, there were 9 loading cycles in

total for each test.

As has been explained on the benefit of the pre-strain, the super-elastic alloy bars were

also pre-strained to 1% and 3% strain levels using the nut of the connection system. The

pre-strained connection conditions were only tested at a weight of 1000kg.

3.   Results and discussions

3.1 Dou-Gong set with conventional wooden peg connections

The results of the Dou-Gong set with conventional wooden peg connections can be illustrated

using moment versus rotation curves. The curves in Figure 10 represent three stages of

stiffness under a 1000kg roof weight. The first is a high elastic stage with a stiffness of

900kNm/rad. During the second, plastic stage the wooden peg of base Dou starts to pull out

from the chiselled hole. The structure then begins to tip over and the lateral load is then

decreased during the third stage of stiffness, the limit stage. Because the Dou-Gong has a

good re-centring capability, the structure then rotated back to its original position without

significant residual displacement after the lateral loads were removed.

The restoring moment of the Dou-Gong set can be calculated using the equation:

$$M = \frac{W \times g \times \cos\theta}{2000L}(L^2 - 2aL - 2LH \times \tan\theta) \tag{1}$$

The parameters are illustrated in Figure 11.

The second level of the structure was assumed to be a rigid frame as there were four Dou

connected to the lower structure which restrained the movement of the upper lever structure.

The restoring moment model at a weight of 1000kg is shown in Figure 10. The stiffness was

virtually the same for both the model and the test results. The difference in level occurs

because, in a practical situation, the upper level structure gives a constant moment to the entire

Dou-Gong set.

Only the hysteresis loops in the first loading cycle with the same rotation angle are shown

in Figure 12 because there was negligible change at a weight of 1000kg (Figure 10). Although

the increased weight on top of the structure will increase the horizontal resistance of the

Dou-Gong set, it will ultimately result in a lower resistance once the Dou-Gong system reaches

the displacement where P-Delta effect needs to be considered. This is shown clearly in Figure

12 when the weight increased to 1000kg. Therefore, a heavier roof means there is a higher risk

of tipping for a historical timber structure with conventional wooden peg connections in an

12

event of earthquake.

3.2 Dou-Gong set with metal bar connections

In this study, two metallic materials, high strength steel and super-elastic alloy, were substituted for the wooden pegs. The vertical loads and the loading schemes remained the same.

The Dou-Gong set with high strength steel bar connections still retained a good self-centring capability. It recovered to its original position after the lateral loads were removed, even when the steel bars were yielded or fractured. The area within the hysteresis loops of the first loading cycle was much larger than in the other two loading cycles (Figure 13). This demonstrated that the Dou-Gong set with high strength steel bar connections dissipated a large amount of energy in the first loading cycle and exhibited a substantial decrease in the next two loading cycles under the same rotation angle. This is because the steel bar entered its plastic stage and showed permanent deformation during the first loading cycle. With the vertical load there is no significant change in the ultimate strength of the Dou-Gong set with high strength steel bar connections.

The super-elastic alloy bar connections give the Dou-Gong set a lower ultimate strength than the high strength steel bar connections, however, this is still much higher than for conventional wooden pegs. The Dou-Gong set experienced four stages of stiffness as shown in Figure 14. The first two stages relate to the stiffness of the Dou-Gong itself while the third and fourth stages come from the super-elastic alloy bars. The shapes of the hysteresis loops under the same rotation angle remain almost the same due to the super-elasticity of the super-elastic

13

alloy bars. The ultimate strength of the Dou-Gong set with super-elastic alloy bar connections increases significantly with the weight on top (as illustrated in Figure 15). A heavier roof will therefore give higher ultimate strength to the Dou-Gong set. The stiffness of the Dou-Gong does not vary with the weight of the roof.

As Figure 16 shows, the second stiffness of Dou-Gong with high strength steel bar connections matched the stiffness of Dou-Gong with conventional wooden peg connections. The high strength steel bars did not exert any effort on the structure at this stage as the material experienced permanent deformation after the first loading cycle and must undergo the low stiffness stage, which is almost zero, from the second loading cycle (Figure 17). However, there was no noticeable change in the first and subsequent loading cycles when using the super-elastic alloy bar.

The equivalent damping ratios (ζ) for each loading case can be calculated using the equation below (Priestley, 1996):

$$\zeta = \frac{A_h}{4\pi \times A_e} \tag{2}$$

The Dou-Gong with high strength steel bar connections gave equivalent damping ratios ranging from 5% -10% in the first loading cycle which reduced to 4% - 6% in the second and third cycles. The super-elastic alloy gave equivalent damping ratios between 7% and 10% with a slight decrease in the second loading cycle (but still higher than 7%) which remained the same in the third loading cycle. These data are presented in Figure 18 and the condition for each test is shown in Table 2. It is possible that, when using a high strength steel bar, the equivalent damping ratio rises when the rotation angle increases. However, the steel will be

14

fractured easily as it already has a permanent deformation, as shown in test 5. There was no indication that the equivalent damping ratios changed with the rotation angle of Dou-Gong when super-elastic alloy bar connections were used.

An earthquake always gives the structure more than one loading cycle and there are several small aftershocks that structures need to overcome. A super-elastic alloy is therefore more suitable for seismic applications than high strength steel because the latter will be damaged during a major earthquake and can provide neither sufficient stiffness nor good damping for the structure when it is subjected to small aftershocks.

3.3 Effects of pre-strained super-elastic alloy

The material tests and single Dou tests all show that the pre-strain of super-elastic alloy could provide a better damping ratio and dissipate more energy. In this research, the pre-strain levels of 1% and 3% were also applied to the super-elastic alloy bar connections.

The equivalent damping ratio of "no pre-strain" loading cases (tests 7-9) already showed a high equivalent damping ratio ranging from 7% to 9% (Figure 19). Figure 20 also shows that "no pre-strain" loading cases gave a higher equivalent damping ratio than the pre-strain loading cases. However, the hysteresis loops show that the 3% pre-strain loading cases dissipated more energy and have higher stiffness than both "no pre-strain" and 1% pre-strain cases. The "no pre-strain" loading cases gave a high equivalent damping ratio under rotations of more than 0.05 radians. They reached the super-elastic stage and the material then showed the super-elasticity effect until the Dou-Gong set rotated to 0.02 radians. The Dou-Gong set only retains its original stiffness and the elastic stiffness of super-elastic alloy under small

15

displacements. The pre-strain of the super-elastic alloy allows the material to have initial super-elasticity and to dissipate a certain amount of energy, even under small displacements.

There are two possible reasons why a two-tiered Dou-Gong set under "no pre-strain" loading cases gave a higher equivalent damping ratio than pre-strain loading cases. The first is that pre-strain loading cases have a higher final stiffness than "no pre-strain" cases. A higher moment is therefore needed to achieve the same rotation angle. Hence, A_e, the maximum elastic strain energy in one loading cycle used to calculate the equivalent damping ratio, will be higher and thus the final equivalent damping ratio will be smaller. The other reason may be that the top tier consists of several components and the movements between these can also dissipate energy. However, the pre-strain of the upper tie connections bound the components tightly together and resisted any movement between them. Therefore, the pre-strain on the super-elastic alloy connection of base Dou and the upper tier is the area that requires further investigation.

Like the "no pre-strain" loading cases, the ultimate strength increases with the top loads applied on the Dou-Gong set in the pre-strain loading cases. The 3% pre-strain of the super-elastic alloy gave a slightly greater ultimate strength than the 1% pre-strain. There are only two stages of stiffness in the Dou-Gong set with 1% pre-strain super-elastic alloy connections. Three stages of stiffness can be observed in the 3% pre-strain loading cases. The structure entered its third stage of stiffness when it was rotated more than 0.05 radians because the super-elastic alloy transferred to its elastic deformation of detwinned martensite.

The equivalent damping ratio of 3% pre-strain loading cases is always higher than 1%

16

pre-strain loading cases (Figure 21). The equivalent damping ratio of the latter ranges from 5%
to 7% and   the former from 6% to 9%. The equivalent damping ratio slightly decreases in the
second and third loading cycles under 3% loading cases but not in the 1% loading cases. The
equivalent damping ratio is also independent of the rotation angle of the Dou-Gong set with
pre-strain super-elastic alloy bar connections.

4. Conclusions

This study used glulam to replicate a full scaled Dou-Gong system deriving from a historical
timber building in Sichuan Province in China. High strength steel and super-elastic alloy were
used as substitutes for conventional wooden peg connections. Push-over tests were then
conducted using a hydraulic jack. This technique addresses the needs of the cases which
involve dismantling, repair and strengthening on those traditional timber structures with
Dou-Gong system. This technique is also reversible when the Dou-Gong system can be
dismantled in the future. The following conclusions can therefore be drawn:

- The ultimate strength increased rapidly with the weight applied on top of the structure
  when conventional wooden peg connections were used. This is because the wooden
  peg was pulled out from the hole without any damage and the lateral load generally
  overcame the weight on top. The P-Delta effect had a higher impact when the weight
  on top was greater, resulting in lower stiffness of the Dou-Gong set.

- Both high strength steel and super-elastic alloy give the Dou-Gong system much
  higher ultimate stiffness than that would be provided by conventional wooden peg
  connections. The high strength steel bar connections provided the Dou-Gong system

17

with the highest equivalent damping ratio and stiffness but only in the first loading cycle. In the second and third loading cycles, the structure experienced a stage of near zero stiffness before reaching ultimate strength due to the permanent deformation of the steel bar. The high strength steel bar thus has a higher risk of fracture during repeated loading cycles.

- Four stages of stiffness were observed in the "no pre-strain" loading cases of a Dou-Gong system with super-elastic alloy bar connections. The first two stages are regarded as the stiffness of the Dou-Gong system itself and the latter two stages are the stiffness of the super-elastic alloy. The first two stages disappeared when pre-strain was applied to the super-elastic alloy bars. The super-elastic alloy with 3% pre-strain showed hysteresis loops with a greater area than "no pre-strain" loading cases; this means it can dissipate more energy. The higher pre-strain level can thus provide the Dou-Gong structure with a higher equivalent damping ratio.

18

References

Chang WS and Hsu MF (2005) Mechanical Characteristics of Traditional Go-Douand Stepped

Dovetail Timber Connections in Taiwan. Taiwan Journal of Forest Science, 20(1): 61-71.

Fang DP, Iwasaki S, Yu MH et al (2001a) Ancient Chinese timber architecture. I:

Experimental study. Journal of Structural Engineering, **127(11)**: 1348-1357.

Fang DP, Iwasaki S, Yu MH et al (2001b) Ancient Chinese Timber Architecture. II: Dynamic

Characteristics. Journal of Structural Engineering, **127(11)**: 1358-1364.

Fujita K, Hanazato T and Sakamoto I (2004), Earthquake Response Monitoring and Seismic

Performance of Five Storied Timber Pagoda. In Proceedings of the 13th World

Conference on Earthquake Engineering.Vancouver, Canada. Paper No 54.

Suzuki Y and Maeno M (2006) Structural mechanism of traditional wooden frames by

dynamic and static tests. Structural Control and Health Monitoring, **13(1)**:508-522.

Yu MH, Oda Y, Fang DP et al (2008) Advances in structural mechanics of Chinese ancient

architectures. Frontiers of Structural and Civil Engineering, **2(1)**:1-25.

Xue J, Wu Z, Zhang F et al (2015) Seismic Damage Evaluation Model of Chinese Ancient

Timber Buildings. Advances in Structural Engineering, 18(10):1671-1683.

Chang WS, Hsu MF and Komatsu K (2006) Rotational performance of traditional Nuki joints

with gap I: theory and verification. Journal of Wood Science, 52(1):58-62.

Chang WS and Hsu MF (2007) Rotational performance of traditional Nuki joints with gap II:

the behavior of butted Nuki joint and its comparison with continuous Nuki joint. Journal

of Wood Science, 53(5):401-407.

19

Chang WS (2005) On rotational performance of traditional Chuan-Dou timber joints in Taiwan. PhD Thesis, National Cheng Kung University, Tainan, Taiwan.

Chang WS, Shanks J, Kitamori A et al. (2009) The structural behaviour of timber joints subjected to bi-axial bending. Earthquake Engineering and Structural Dynamics. **38(6)**: 739-757.

Yeo SY, Komatsu K, Hsu MF et al. (2018) Structural behavior of traditional Dieh-Dou timber main frame. International Journal of Architectural Heritage. **12(4)**: 555-577.

Xie W, Araki Y and Chang WS (2018) Enhancing the seismic performance of historic timber buildings in Asia by applying super-elastic alloy to a Chinese complex bracket system. International Journal of Architectural Heritage. **12(4)**: 734-748.

Chang WS and Araki Y (2016) Use of shape-memory alloys in construction: a critical review. Proceedings of the Institution of Civil Engineers - Civil Engineering, 169 (2): 87-95.

Fujita K, Sakamoto I, Ohashi Y. et al (2000) Static and dynamic loading tests of bracket complexes used in traditional timber structures in Japan. In Proceedings of the 12th World Conference on Earthquake Engineering. New Zeland. Paper No 0851.

Tsuwa I, Koshihara M, Fujita K et al. (2008) A Study on the Size Effect of Bracket Complexes Used in Traditional Timber Structures on the Vibration Characteristics. In Proceedings of the 10th World Conference in Timber Engineering, Miyazaki, Japan.

Fujita K, Chiba K, Kawai N et al. (2008) Earthquake response analysis of traditional Japanese timber pagoda. In Proceedings of the 10th World Conference on Timber Engineering, Miyazaki, Japan.

Hwang JK, Hong SG, Kim NH et al (2008) The effect of friction joint and Gongpo (bracket set) as an energy dissipation in Korean traditional wooden structure. In *Structural Analysis of Historic Construction* (D'Ayala D & Fodde E (eds)). pp. 861-866.

Yeo SY, Hsu MF, Komatsu K, et al. (2016a) Shaking Table Test of the Taiwanese Traditional Dieh-Dou Timber Frame. International Journal of Architectural Heritage. **10(5)**: 539-557.

Yeo SY, Komatsu K, Hsu MF et al (2016b) Mechanical model for complex brackets system of the Taiwanese traditional Dieh-Dou timber structures. Advances in Structural Engineering, 19(1): 65-85.

Priestley MJN, Seible F and Calvi GM (1996). Seismic design and retrofit of bridges. New York: John Wiley.

21

Table 1. Mechanical properties of Glulam GL28h

Mean modulus of elasticity ($E_{0,mean}$)	12600N/mm^2
Mean modulus of elasticity perp. to grain ($E_{90,mean}$)	420N/mm^2
Bending strength ($f_{m,k}$)	28N/mm^2
Tension strength ($f_{t,0,k}$)	19.5N/mm^2
Compression strength ($f_{c,0,k}$)	26.5N/mm^2
Compression strength perp. to grain ($f_{c,90,k}$)	3.0N/mm^2

22

Table 2. Test protocol

Test No.	Material for Connection	Weights on top	Pre-Strain
1	Wooden Peg	400kg	N/A
2	Wooden Peg	700kg	N/A
3	Wooden Peg	1000kg	N/A
4	Steel Bar	400kg	N/A
5	Steel Bar	700kg	N/A
6	Steel Bar	1000kg	N/A
7	SEA Bar	400kg	None
8	SEA Bar	700kg	None
9	SEA Bar	1000kg	None
10	SEA Bar	400kg	1%
11	SEA Bar	700kg	1%
12	SEA Bar	1000kg	1%
13	SEA Bar	400kg	3%
14	SEA Bar	700kg	3%
15	SEA Bar	1000kg	3%

23

Figure 1. Location of Dou-Gon system and its formation (Xie W, Araki Y and Chang WS, 2018)

24
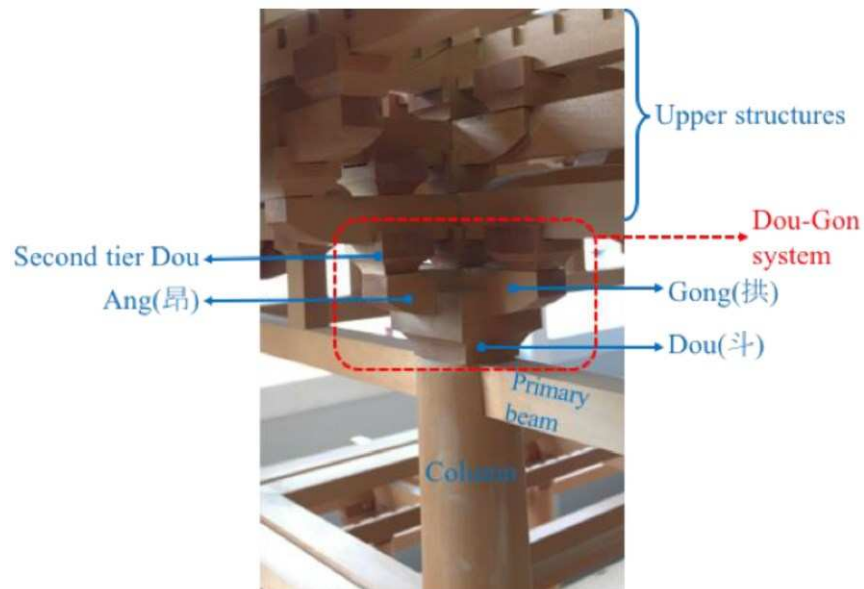
Figure 2. 3D drawing of elements in Dou-Gon system
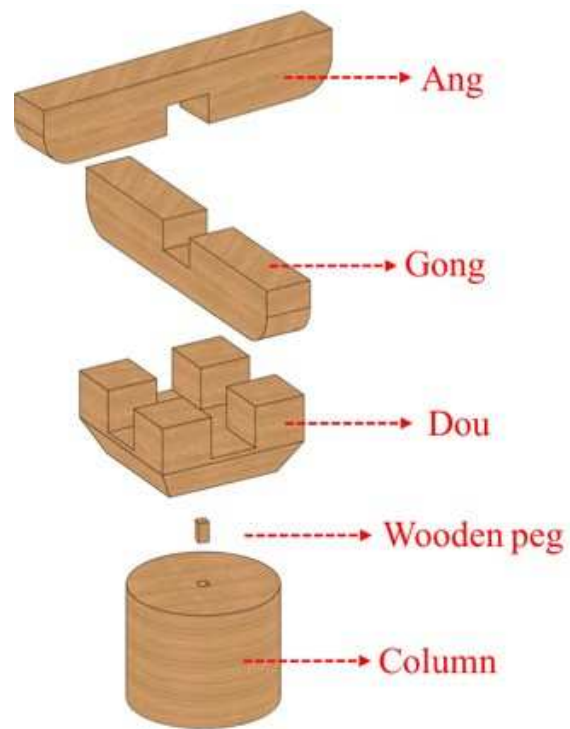
Figure 3. Bar connection for base Dou with dimensions, upper: high strength steel; lower: super-elastic alloy (Xie W, Araki Y and Chang WS, 2018)

26
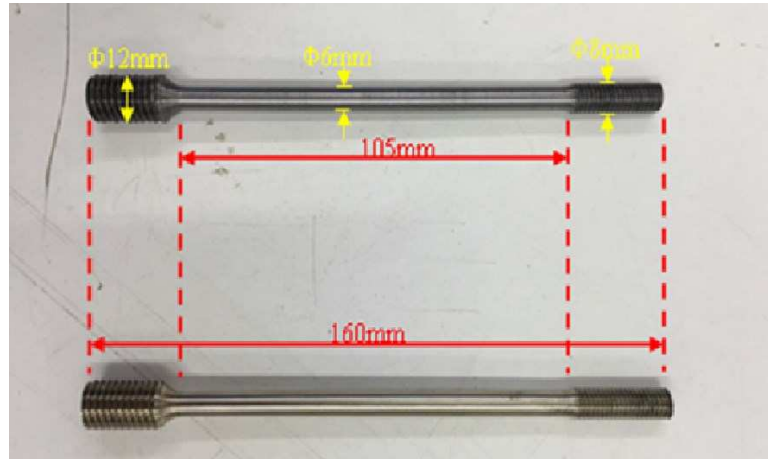
Figure 4. The different phases of SEA at different temperatures, and its relationship with the shape memory and super-elasticity effects (Chang & Araki, 2016)

27
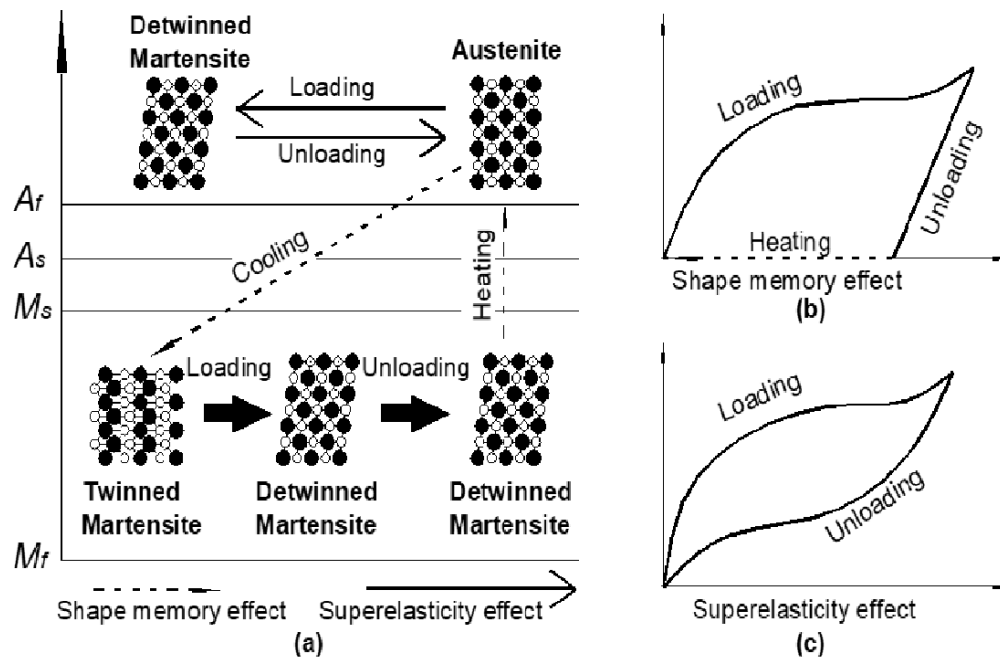
Figure 5. Schematic of pre-strain on super-elastic alloy
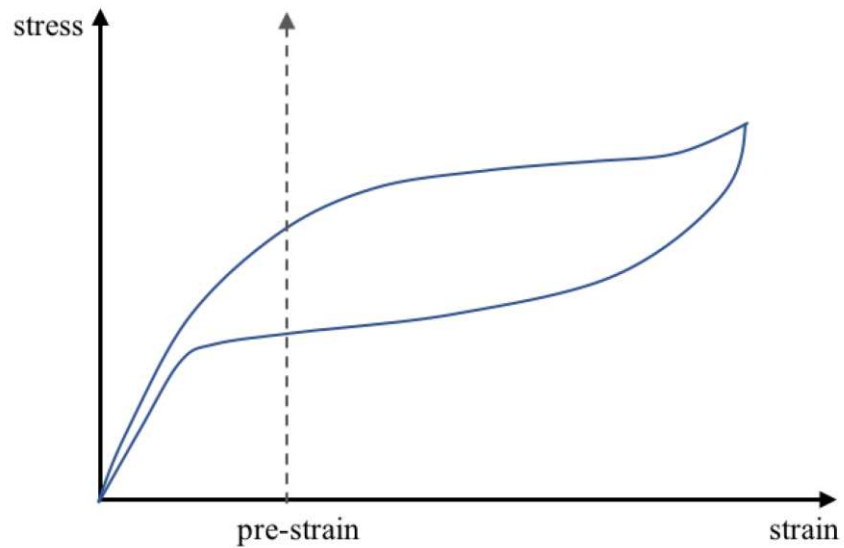
Figure 6. Stress-strain curves of metal bars (Xie W, Araki Y and Chang WS, 2018)
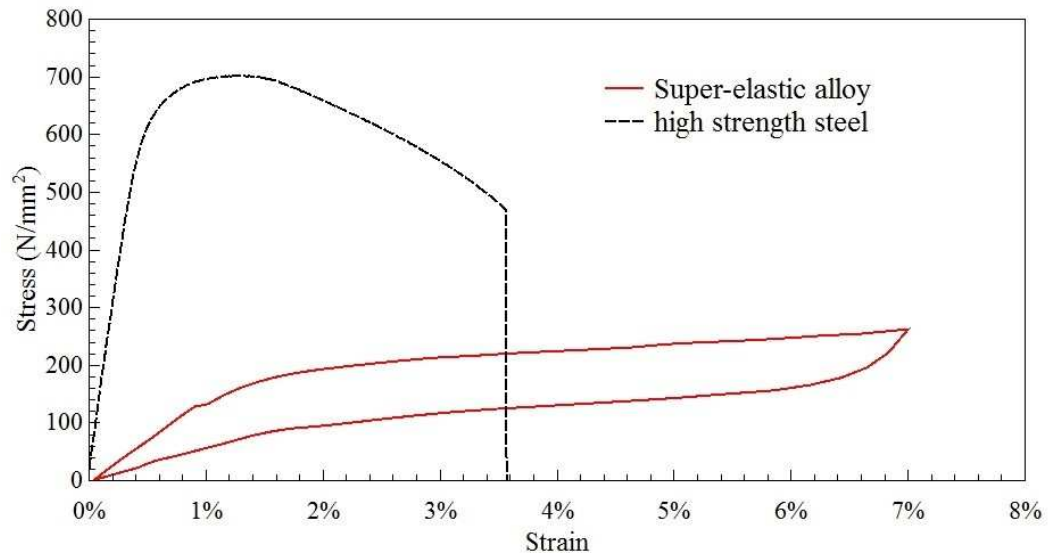
Figure 7. (a) 3D exploded view drawing of Dou-Gon; (b) and (c) Dou-Gon set up without dead loads
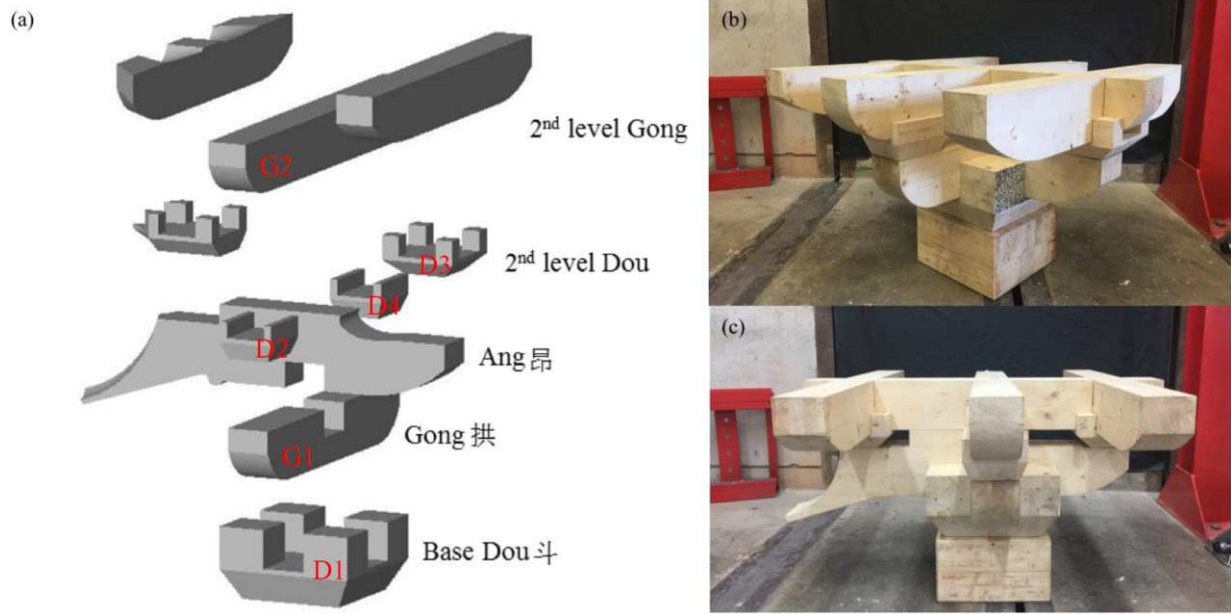
Figure 8. (a) 12mm thread insert; (b) Square plate and ball joint; (c) Details of metal bar connection (Xie W, Araki Y and Chang WS, 2018)
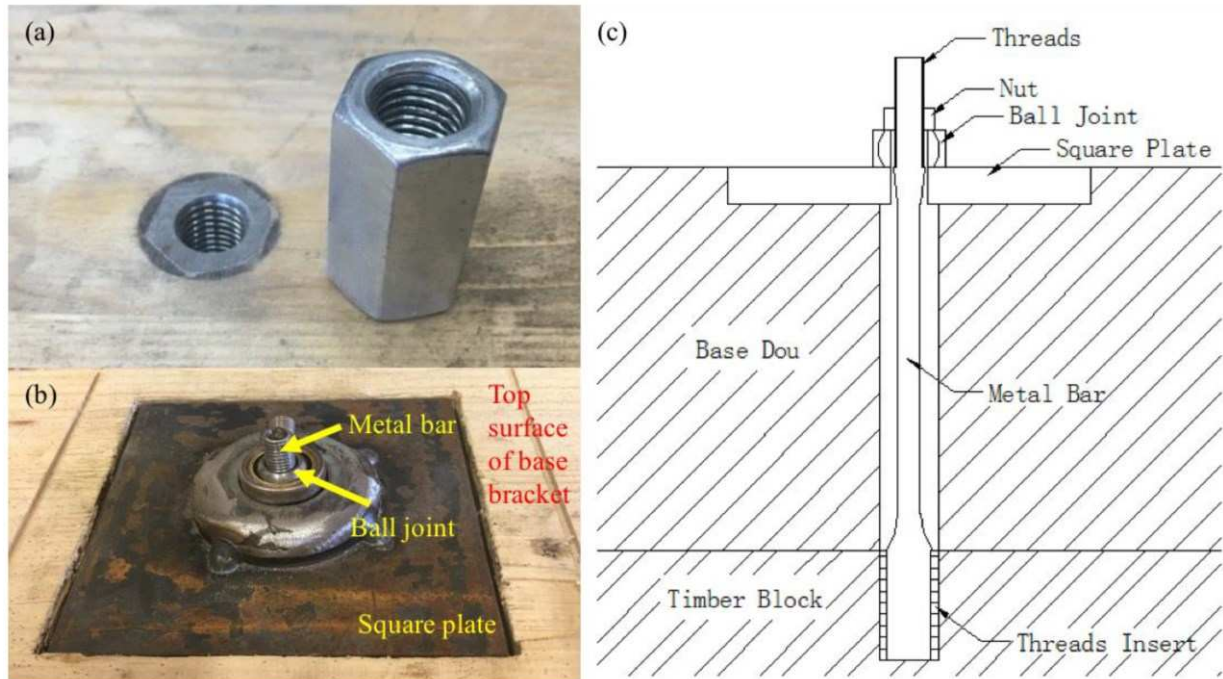
Figure 9. Loading apparatus and instrumentation (Xie W, Araki Y and Chang WS, 2018)

32
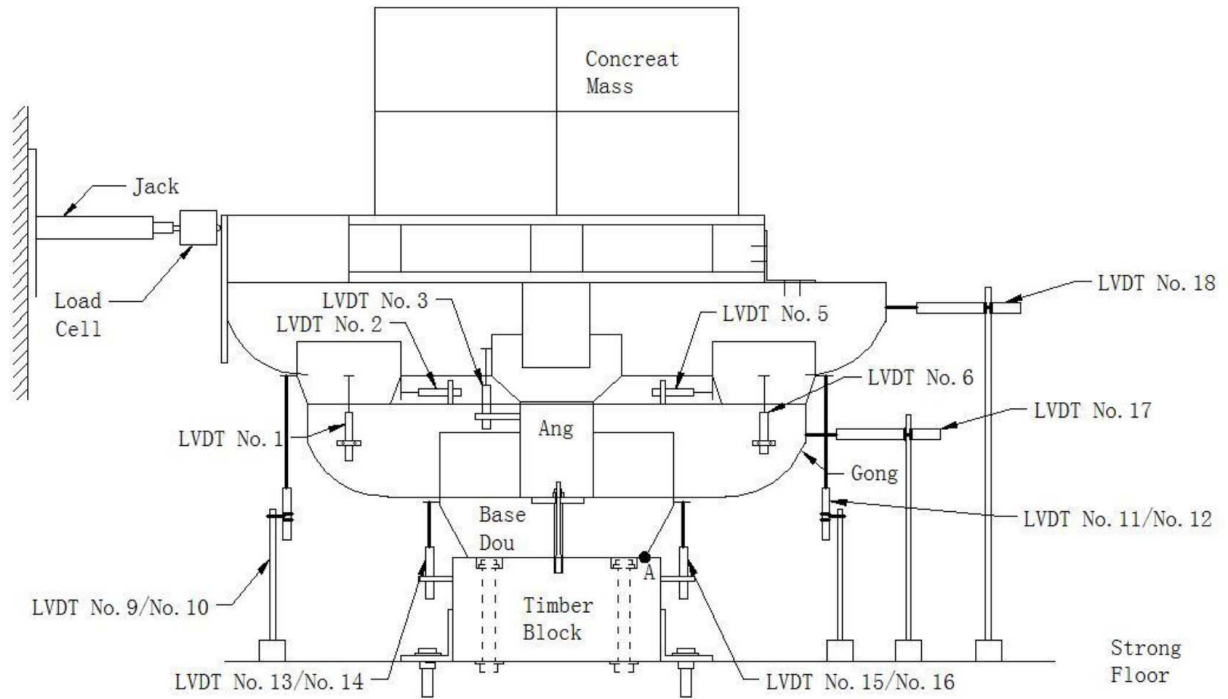
Figure 10. Hysteresis loops of Dou-Gon set with wooden peg connections at a weight of 1000kg
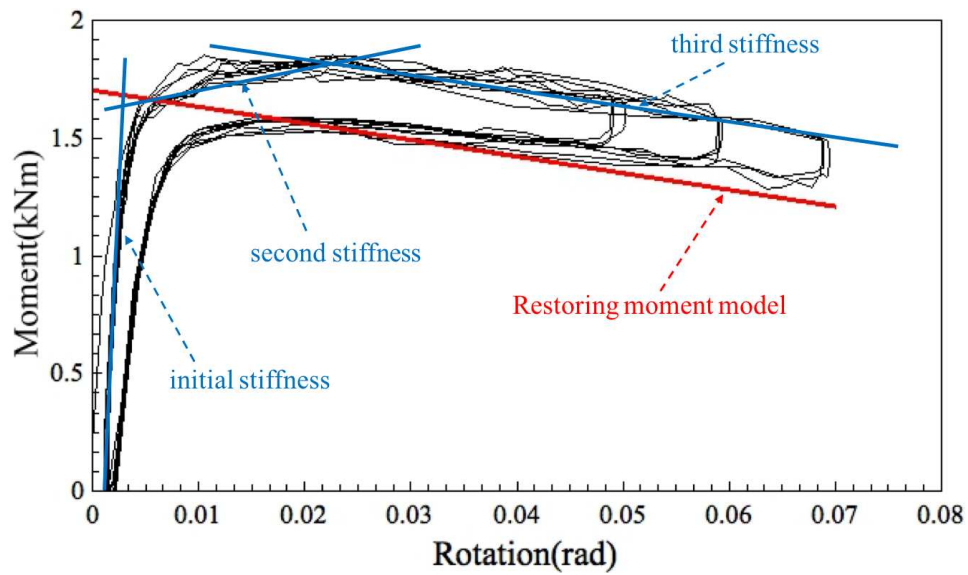
Figure 11. Simplified model of the structure and loadings
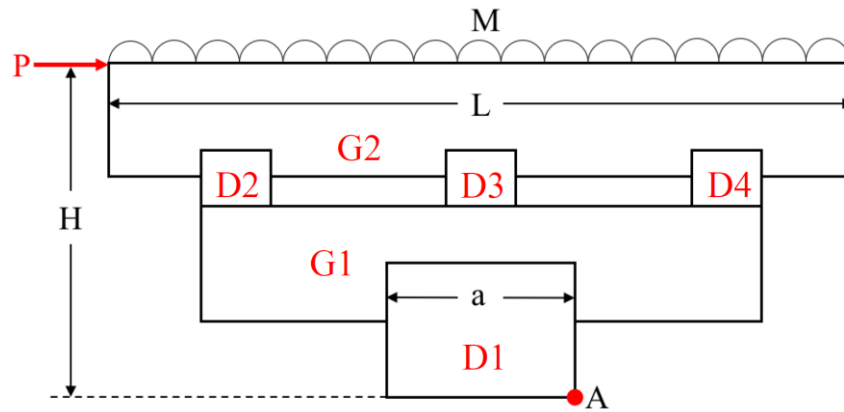
Figure 12. Hysteresis loops of Dou-Gon set with wooden peg connections under different weights

35
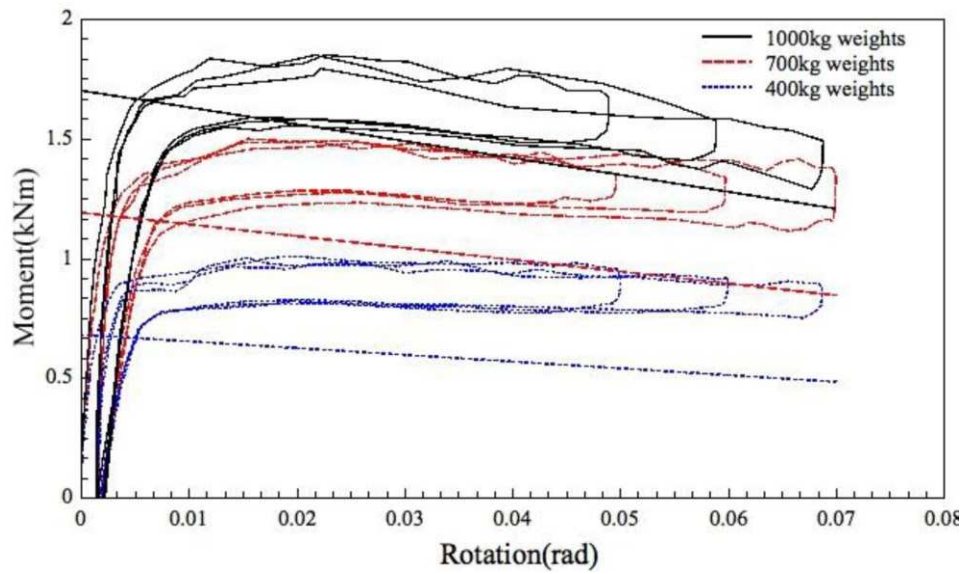
Figure 13. Hysteresis loops of Dou-Gon set with high strength steel bar connections
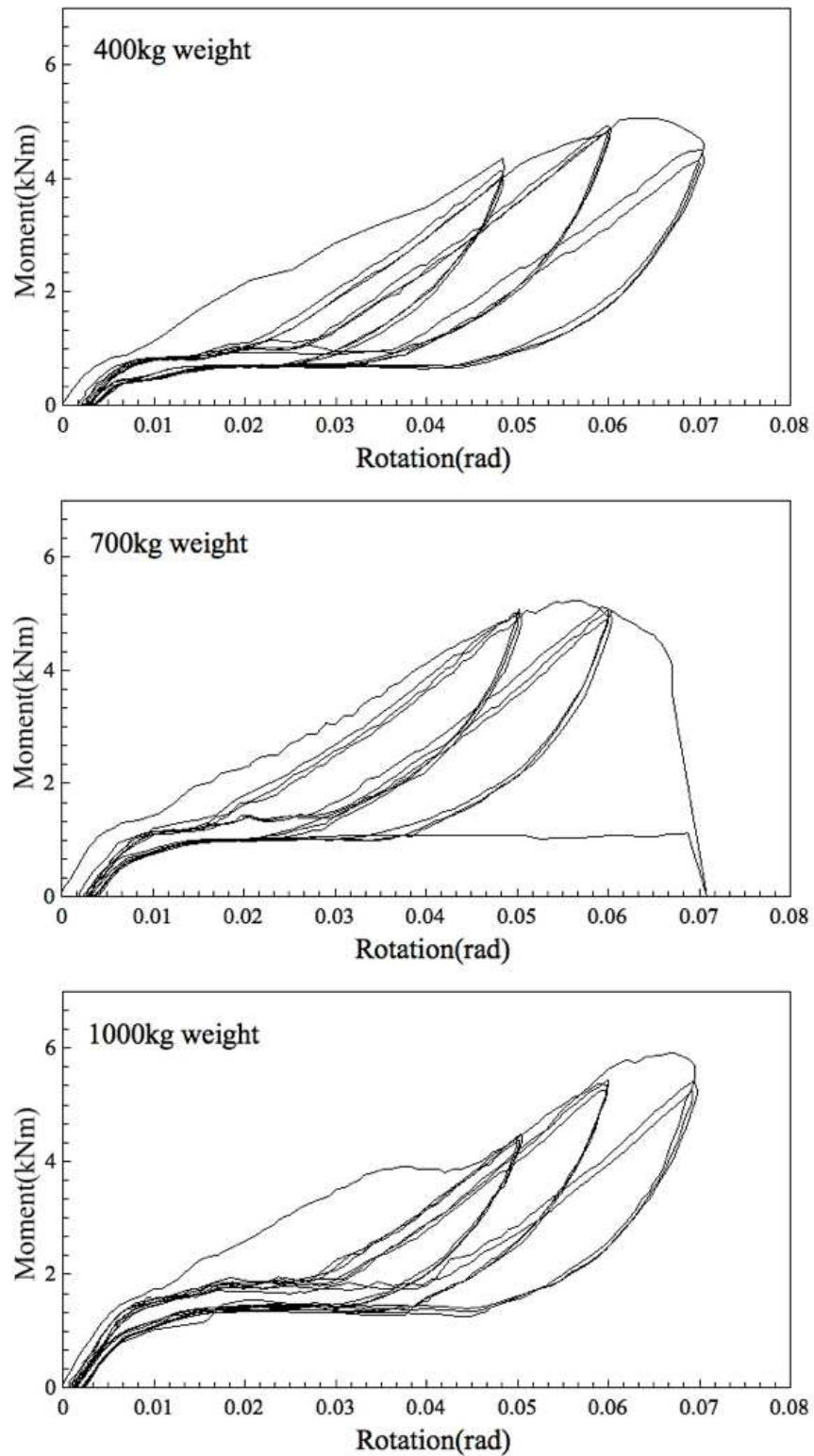
Figure 14. Hysteresis loops of Dou-Gon set with super-elastic alloy bar connections at a weight of 1000kg
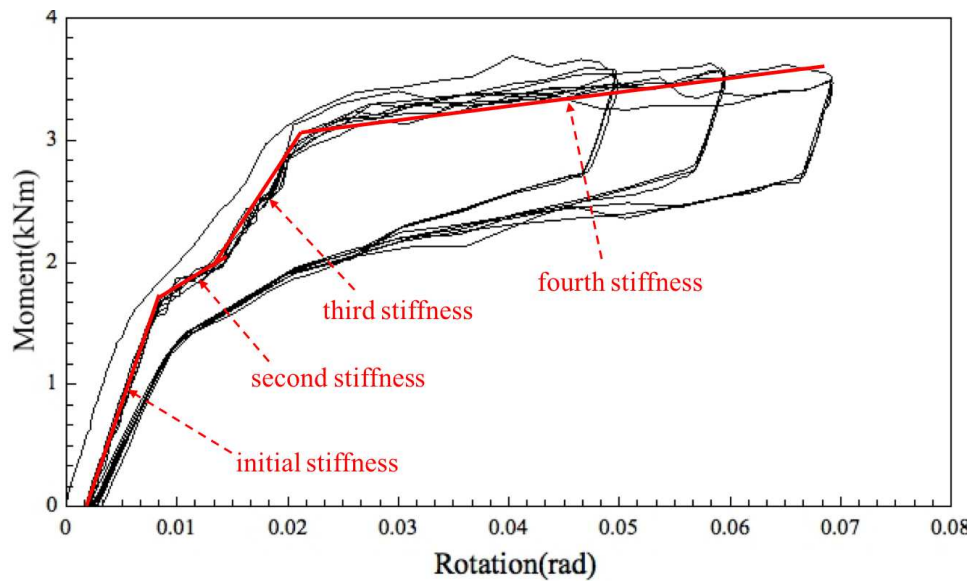
Figure 15. Hysteresis loops of first cycle of each rotation step for Dou-Gon set with super-elastic alloy bar connections
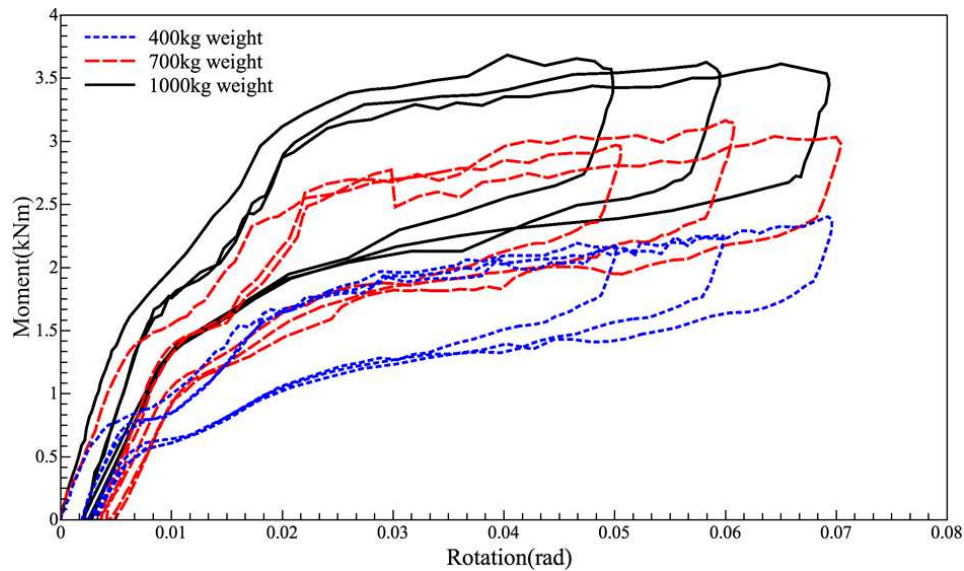
Figure 16. Comparison of three different connection materials at a weight of 1000kg
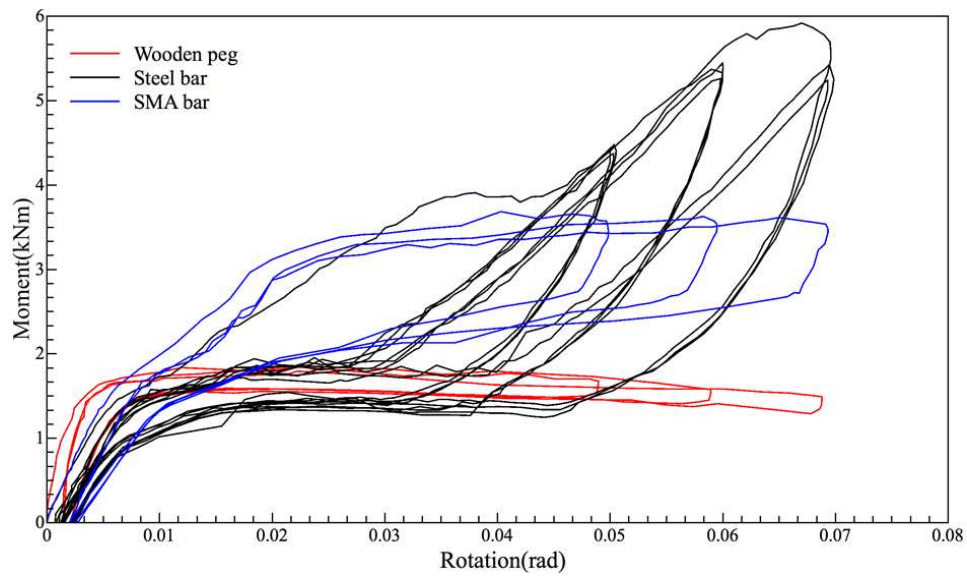
Figure 17. Schematic illustration of first two loading cycles of Dou-Gon connected by (a) high strength steel bar and (b)super-elastic alloy bar (Xie W, Araki Y and Chang WS, 2018)
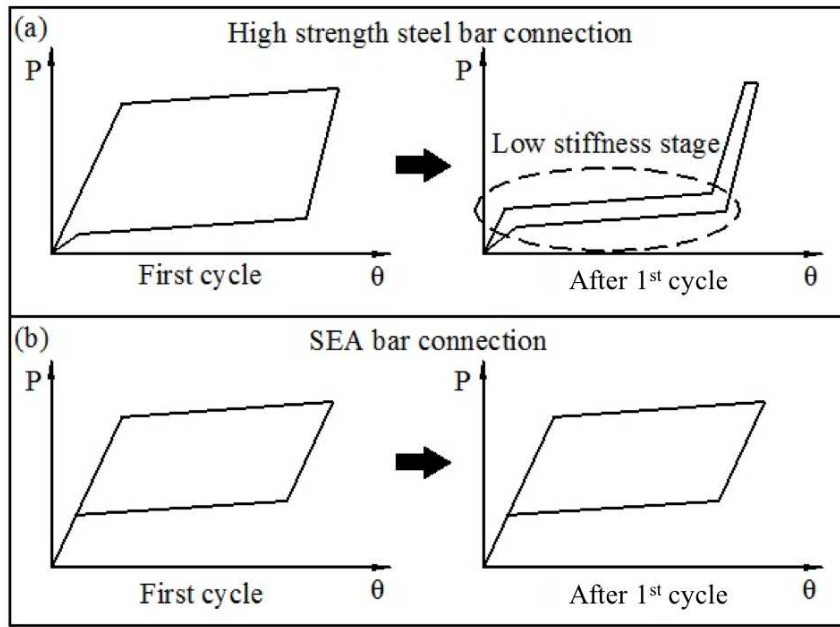
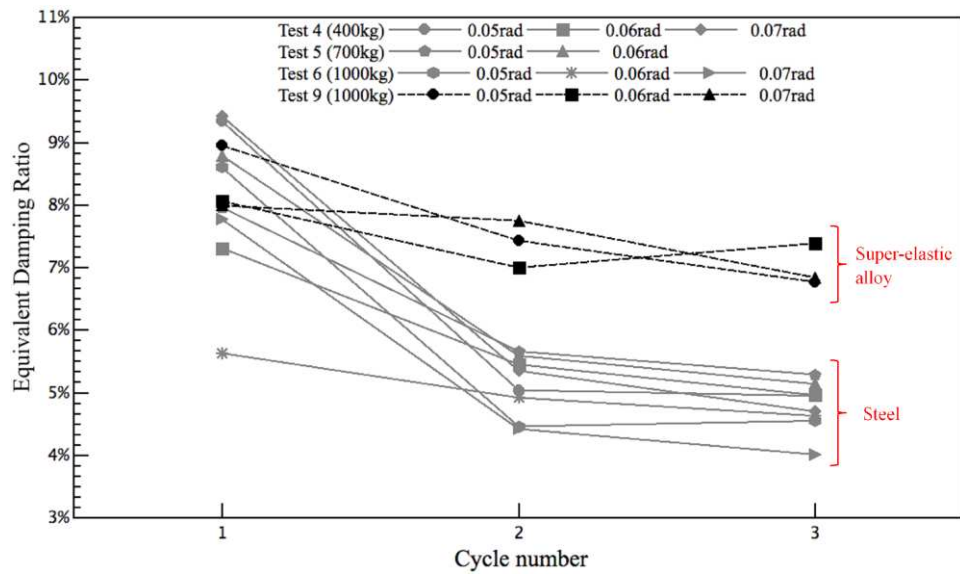**Figure 18.** Equivalent damping ratios change with loading cycle

Figure 19. Equivalent damping ratios change with roof weight
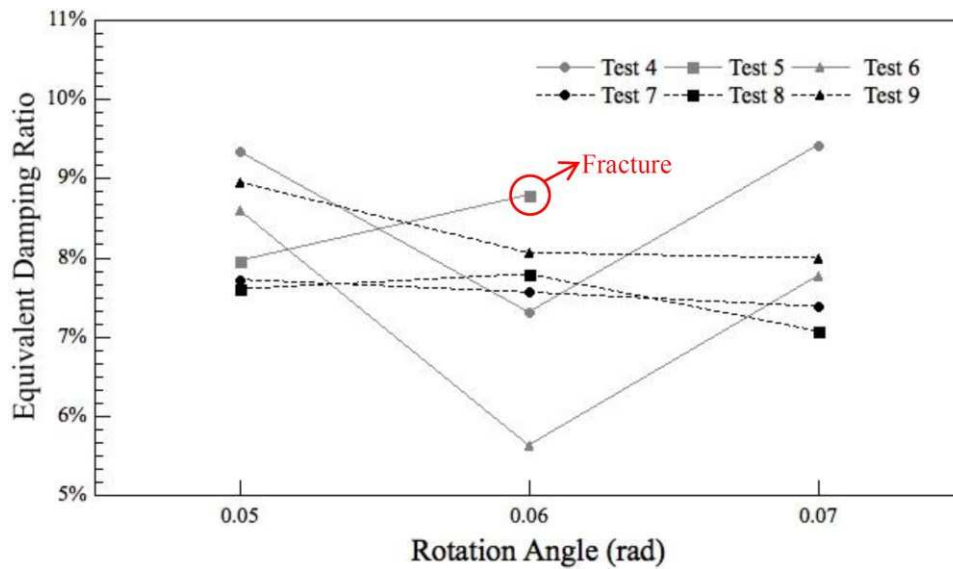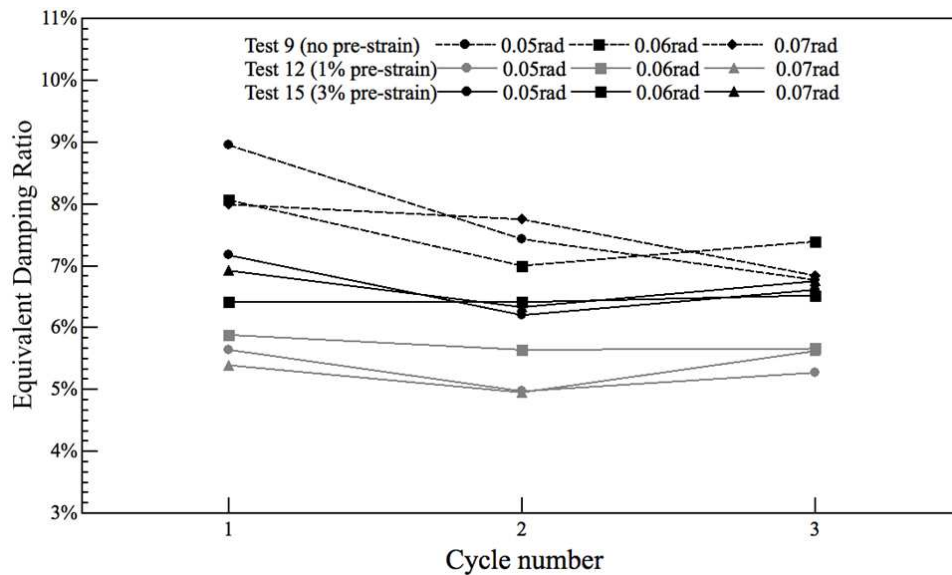
Figure 20. Equivalent damping ratios change with the pre-strain level of super-elastic alloy

Figure 21. The effect of top loads on the equivalent damping ratio of Dou-Gon with super-elastic alloy pre-straining to (a) 1% strain level; (b) 3% strain level

44